PHILOSOPHICAL TRANSACTIONS A

royalsocietypublishing.org/rsta

CC BY

Review

Cite this article: Kant R, Soni H, Gupta RK, Sood AK, Ramaswamy S. 2026 Antidiffusive instabilities in active matter: granular experiments, theory and outlook. *Phil. Trans. R. Soc. A* **384**: 20250137.
https://doi.org/10.1098/rsta.2025.0137

Received: 16 March 2026
Accepted: 20 July 2026

One contribution of 14 to a theme issue 'Anti-diffusive transport and layering: from sub-cellular to astrophysical scales'.

Subject Areas:
statistical physics, complexity

Keywords:
active matter, non-equilibrium systems, phase separation and antidiffusion

Author for correspondence:
Sriram Ramaswamy
e-mail: sriram@iisc.ac.in

Antidiffusive instabilities in active matter: granular experiments, theory and outlook

Raushan Kant[1,2], Harsh Soni[3], Rahul Kumar Gupta[4], Ajay Kumar Sood[1] and Sriram Ramaswamy[1,5]

[1]Department of Physics, Indian Institute of Science, Bengaluru 560 012, Karnataka, India
[2]Institute of Science and Technology Austria, 3400 Klosterneuburg, Lower Austria, Austria
[3]Department of Physics, Indian Institute of Technology Mandi - Kamand Campus, Mandi 175 005, Himachal Pradesh, India
[4]Sankhyasutra Labs Ltd., Manyata Embassy Business Park, Bengaluru 560 045, Karnataka, India
[5]International Centre for Theoretical Sciences, Tata Institute of Fundamental Research, Bengaluru 560 089, Karnataka, India

SR, 0000-0001-7726-8556

This article presents a perspective on the widespread occurrence of antidiffusive instabilities in systems in which free energy is supplied in a sustained manner directly to the constituent particles. Defining this distinct category allows a discussion of living matter as a special kind of non-equilibrium material. After an introduction surveying diverse manifestations of antidiffusion, including some in which momentum transfer through an ambient fluid plays a central role, we describe experiments and theory on a striking and extreme form that arises in a vibrated monolayer of macroscopic particles. This article has two aims: to bring active matter as a novel hydrodynamic arena to the attention of researchers in large-scale fluid and plasma flows, and to highlight open issues arising in our work with wider implications for a statistical thermodynamics of active matter.

This article is part of the theme issue 'Anti-diffusive transport and layering: from sub-cellular to astrophysical scales'.

© 2026 The Authors. Published by the Royal Society under the terms of the Creative Commons Attribution License http://creativecommons.org/licenses/by/4.0/, which permits unrestricted use, provided the original author and source are credited.

THE ROYAL SOCIETY PUBLISHING

Downloaded from royalsocietypublishing.org/rsta/article-pdf/doi/10.1098/rsta.2025.0137/6175896/rsta.2025.0137.pdf
by Institue of Science & Technology Austria user
on 17 November 2026

1. Introduction

(a) Active matter

The emergence of structure in macroscopic systems [1] is often mediated by transport up a gradient, sharpening rather than smoothing an initial inhomogeneity in composition or velocity, for example. We use the term antidiffusion to describe such processes in which a growing mode overcomes normal diffusive relaxation, leading to the spontaneous amplification of fluctuations about a uniform initial state. The ideal use of the term would be when linear stability analysis yields a positive eigenvalue scaling as $\mathcal{O}(q^2)$ to leading order at small wavenumber q of a perturbation [1–3], but that is a matter of taste. This article will present examples of such antidiffusive behaviour in a setting with which researchers working on large-scale flows may not be familiar, namely, self-driven or active fluids. We therefore begin with some essential background. Active matter, by definition, continually converts a sustained free-energy supply into work at the scale of its constituent particles, yielding a wealth of emergent behaviours [4–12] that distinguish it from 'passive' matter at thermal equilibrium. The novelty of this class of systems, which of course includes all living matter, can be seen in unusual ordered phases [13–19], unusual mechanisms for familiar phase transitions [20–23], anomalously large [24] or anomalously small [25–27] fluctuations, counterintuitive mechanical response [28–34] and the destruction of ordered states by activity-driven instabilities [27,35,36]. The last of these provides the engine for the iconic 'active turbulence' at low Reynolds number [37], whose similarities and differences when compared to its inertial counterpart are a subject of continuing interest.

Several of the striking effects referred to above are associated with a change in sign of an effective diffusivity and therefore merit discussion in this thematic issue. The cases discussed are diverse, unified by a common effect rather than a universal cause, but should serve to invite researchers outside our usual orbit to engage with active-matter physics. This article is neither a review nor an announcement of new results, but a perspective with two aims. One is to survey a range of examples of antidiffusion in active-matter systems, to give the reader a sense of its wide occurrence and suggest potential new venues in which to prospect for analogues to phenomena associated with antidiffusion in large-scale flows, such as staircases [38–40] in stratified fluids and magnetized plasmas. These are self-organized step-like profiles of concentration or temperature in which sharp, antidiffusively steepened gradients that suppress transport separate broad regions of turbulent mixing. The second is to dwell at length on one example from our work, in which the non-active-matter reader should find an accessible tabletop realization of antidiffusion and the active-matter researcher should confront fundamental questions in the statistical thermodynamics of phase separation far from equilibrium.

(b) The varieties of active antidiffusion

(i) Swimmers in a viscous fluid

Swimming organisms can be viewed as orientable objects endowed with permanent force dipoles [41]. Indeed, these 'stresslets' determine the leading far-field fluid flow that they generate in an unbounded Stokesian fluid. We will ignore at this stage their swimming speed v_0, as it enters the far-field flow at sub-leading order, but will return to its effect below, when we include fluid inertia, which we ignore for now. A macroscopically aligned state of their orientations, and therefore of their stress, is unstable without a threshold [27,35,36] to buckling along or transverse to the axis of alignment. Perturbations at small wavevector $\mathbf{q}$ about the aligned state evolve at a $|\mathbf{q}|$-independent rate $\propto \cos 2\theta\, cW/\eta$, where θ is the angle between $\mathbf{q}$ and the axis of alignment, c is the particle concentration, W is the strength of their intrinsic force dipoles and η is the shear viscosity. This implies a growing mode for θ below or above 45° for $\mathrm{sgn}W = +1$ ('pushers') or -1 ('pullers'), respectively. Stabilizing contributions $\propto (K/\eta)q^2$, where K is a typical orientational elastic constant,

Downloaded from royalsocietypublishing.org/rsta/article-pdf/doi/10.1098/rsta.2025.0137/6175896/rsta.2025.0137.pdf
by Institue of Science & Technology Austria user
on 17 November 2026

enter at next order in q but cannot avert the small-q instability. Pedantically speaking, the defeat of diffusive relaxation by an instability with a wavenumber-independent growth rate is not precisely antidiffusive, so consider instead the same suspension between planar no-slip walls separated in the y direction by a distance b. Confinement screens the Stokesian hydrodynamic interaction on scales larger than b in the unbounded xz plane, force dipoles and nematic elasticity compete on an equal footing, and the orientational relaxation rate is now $\sim (cWb^2 \cos 2\theta - K)q^2/\eta$. A manifestly antidiffusive instability then arises if the 'active stress' [35] $cW > K/b^2$. For details and subtleties see [42] and [43]. In isotropic suspensions of pusher swimmers, feedback between active flow and flow-induced alignment can lead to zero or negative effective viscosities [44–46], which is classic antidiffusion. Swimmer suspensions with an imposed and immutable uniaxial orientation display their own type of antidiffusion—as well as superdiffusion—through the transport of concentration fluctuations by the active flow they themselves create [47].

(ii) Inertia, motility and antidiffusion

Suspensions of swimmers with non-negligible Reynolds number at the particle scale display their own distinctive varieties of antidiffusion. When mechanical inertia in the form of the suspension mass density ρ is taken into account, the single time constant η/cW of the Stokesian instability of §1b(i) above is replaced [35,48], at asymptotically small wavenumbers q, by a rate approximately $(cW/\rho)^{1/2}q$ of exponential growth linear in q. The proportionality constant $(cW/\rho)^{1/2}$ relates the time for the amplitude of a disturbance to grow by a factor of e to the length scale $1/q$ on which the disturbance occurs, and is thus the *invasion speed* of the instability. The long-time state in the regime in which this instability dominates is found numerically to be hedgehog defect turbulence [48]. This instability mechanism experiences competition from self-propulsion, whose speed v_0, if large enough compared to $(cW/\rho)^{1/2}$, allows the system to outswim the instability [48]. The complicated but interesting detail is that as v_0 is increased, the $O(q)$ growing mode first gives way to one with growth rate of $O(q^2)$ before a stable wave-like propagating mode takes over at larger v_0. The unambiguously antidiffusive $O(q^2)$ growth culminates neither in defect chaos nor in layering, but in a noisy yet ordered phase-turbulent state, whose properties are discussed in [48].

In the example just discussed, what antidiffuses are orientation and velocity fields. Antidiffusion of the *concentration* field in a flock, a collectively moving state of orientationally aligned motile particles, was shown [49] to arise even at large v_0 where the instability of [48] is absent. The mechanism is intricate, involving competition between steric and flow-coupled mechanisms for the reorientation of active particles in response to concentration gradients, and both motility and the lag owing to fluid inertia are crucial. The antidiffusively growing excitations travel as concentration waves (figure 1c), transitioning from orderly to chaotic with increasing v_0 [49].

A mechanism for extreme antidiffusive behaviour in suspensions of inertialess motile particles advected by fluid flow and reoriented by its gradients can be found in recent theoretical and numerical studies [51]. The persistent self-propulsion of the particles takes over the role normally played by particle inertia [56], leading to centrifugation out of vortical regions and singular accumulation in the form of caustics in straining regions [51] (figure 1b). The mechanism is quite distinct from those discussed above, as the particles do not affect but only respond to the flow.

The key to antidiffusion in the examples discussed so far has been the organizing effect of the coherent large-scale fluid flow that arose upon disturbing a uniform state. We now make a transition to the type of active matter in which fluid flow does not play a role, and antidiffusion arises through persistent motility.

(iii) Antidiffusion in dry active matter

Collections of motile particles moving through or over an inert medium that serves as a momentum sink, so that there are no interactions mediated by the flow of an ambient solvent, constitute an important class of active materials. These systems, dubbed 'dry' active matter [8],

Downloaded from royalsocietypublishing.org/rsta/article-pdf/doi/10.1098/rsta.2025.0137/6175896/rsta.2025.0137.pdf
by Institue of Science & Technology Austria user
on 17 November 2026

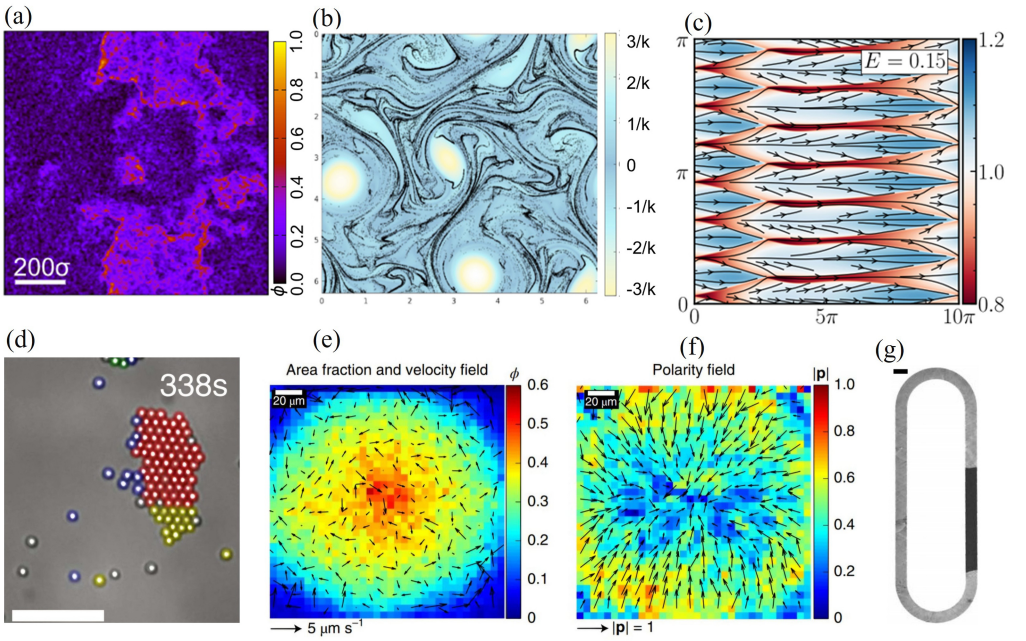


Figure 1. Antidiffusive phenomena across a range of active systems. (a) Active particles induce phase separation in active/passive mixtures, creating dense and dilute passive particle regions with active particles concentrated at interfaces (active particle fraction = 0.25, density plots shown for active particles, adapted from [50]). (b) Aggregation of active swimmers into caustics. Snapshot from a simulation of active, inertialess swimmers (black dots) in a two-dimensional turbulent fluid flow (background vorticity in colour). The swimmers do not remain uniformly distributed but are instead focused by the flow into sharp, filamentary structures of extremely high density, known as 'active caustics'. Here, particle trajectories are systematically collected to create singular concentration gradients from a dilute initial state (adapted from [51]). (c) Antidiffusive concentration-wave formation in an active fluid. Snapshot from a numerical simulation shows particle concentration (colour map) with order parameter streamlines. Starting from a uniform state, the system's collective activity drives the spontaneous formation of stable, travelling concentration waves (adapted from [49]). (d) Colloids self-propelled by light-activated chemistry condense into dense, dynamic crystals, realizing an analogue of chemotactic aggregation [52] through a mechanism combining phoretic attraction and motility-induced phase separation (MIPS) [20] (adapted from [53]). (e) Time-averaged local area fraction overlaid with the velocity field (arrows) for an active cluster of self-propelled Janus colloids. (f) The corresponding polarity field of the same cluster (adapted from [54]). Unlike standard MIPS, these particles experience non-reciprocal torques that orient them inward towards crowded regions. This active propulsion up the density gradient provides a clear, torque-driven mechanism for antidiffusion, resulting in phase separation in which the condensed clusters remain highly fluid. (g) An active solid 'traffic jam' (dark region) steadily propagates through a homogeneous, flowing polar liquid (light region) of Quincke rollers. This phase separation is driven by a standard MIPS mechanism: as particles crowd, near-field interactions physically frustrate their rolling motion. Consequently, the dense phase inherently loses the underlying polar orientational order of the flock (scale bar: 2 mm, adapted from [55]).

abound with antidiffusive behaviour, such as the banded state that intervenes between disordered and uniaxially aligned phases in active systems [10]. Antidiffusive phase separation can also occur within these moving flocks. A classic example of such aggregation is the chemotactic model of Keller & Segel [52], where organisms accumulate via a mediating chemical field. A striking synthetic realization of field-mediated antidiffusion is seen in the 'living crystals' of light-activated colloidal surfers [53], which generate and propel themselves up chemical gradients to condense into dynamic clusters (figure 1d). Building on this, Miller & Toner [57] recently demonstrated that 'autochemotaxis' within a polar flock similarly drives an antidiffusive spinodal decomposition into dense and rarefied bands. Even in the absence of aligning interactions, self-propelled particles can segregate into dense and dilute regions through motility-induced phase

Downloaded from royalsocietypublishing.org/rsta/article-pdf/doi/10.1098/rsta.2025.0137/6175896/rsta.2025.0137.pdf
by Institue of Science & Technology Austria user
on 17 November 2026

separation (MIPS) [20,58–61]. At a coarse-grained level, the effect can be seen as a positive feedback: excluded volume locally slows down self-propulsion in dense regions, which in turn promotes their growth [20,58,59]. Alternatively, consider an incipient densely packed cluster surrounded by vapour at concentration c_v, in a system of impenetrable particles of size a, speed v_0 and rotational diffusivity D_r moving in d space dimensions. Balancing fluxes $v_0 c_v$ into and D_r/a^{d-1} out of the cluster yields an order-unity threshold [61] for Péclet number v_0/aD_r times packing fraction $\phi = ca^d$, above which escape by rotational diffusion of the motility direction is futile because the influx is too large. This simple argument, however, ignores the close-packing upper limit on ϕ, the reduction of effective motility with increasing ϕ and thermodynamic forces not captured by motility reduction, whose broad outcome [20] is a minimum Pe, and a critical point, for this active phase-separation mechanism. MIPS shares many features [20,58–61] with its thermal equilibrium counterpart, including the familiar antidiffusive process known as spinodal decomposition [3]. This crowding-induced slowdown can even drive phase separation within an aligned flock; Geyer *et al.* [55] demonstrated MIPS in a Quincke-roller flock [62], where density-dependent crowding causes particles to jam and inherently lose their polar order (figure 1g). Note, this last system is a suspension, and the motility of its individual constituents relies on an ambient fluid, but its collective behaviour appears to be insensitive to long-range hydrodynamic effects. We therefore mention it in this section on 'dry' active matter.

While standard MIPS relies on density-induced slowdown, Zhang *et al.* [54] present a qualitatively different mechanism, namely, non-reciprocal torques that reorient Janus colloids up a density gradient, providing a clear torque-driven example of antidiffusion where the resulting clusters remain fluid (figure 1e,f).

A qualitatively distinct realization of antidiffusive dynamics of the concentration is predicted to arise as an epiphenomenon during the coarsening of active nematics [63]. The onset of nematic order following a quench from the isotropic phase proceeds in both active and passive systems by the local emergence of nematic regions, each with its own principal axis, whose mutual orientational mismatch is handled by the appearance of topological defects. The growth kinetics is then governed by the attraction and eventual annihilation of oppositely-charged defects. In *active* nematics, however, the orientational distortion around the topological defects drives large-scale curvature-induced particle currents [64], leading [63] to clumping of the density en route to the homogeneous, though fluctuating, final state. Another intriguing manifestation of antidiffusive behaviour has been reported in a vibrated monolayer of tapered, apolar granular rods [65]. At high packing fractions, the tapered shape of the rods gives rise to a chevron phase, characterized by alternating layers in which the rods are slightly tilted in opposite directions with respect to the global nematic director.

Two-dimensional systems in which the constituent particles locomote by transducing the energy of mechanical vibration in the third direction [13,24,66–72] are a convenient and faithful realization of dry active matter, and will serve as the setting for the findings and analysis to which we devote the rest of this article. We will present experimental results on the condensation of a macroscopic passive population by a tiny active minority [73] (see also [50] and [74]) and construct the theory of the spinodal, i.e. the onset of antidiffusion, for this transition. We note that this mechanism for condensation is similar to two-temperature phase separation [15,17]: the motile component, by virtue of a large effective diffusivity thanks to highly persistent self-propulsion, plays the role of the hot species, sequestering the 'cold', i.e. less rapidly diffusing, passive species. We do not pursue here the connections between [73] and the competing spinodal and travelling instabilities in non-reciprocal Cahn-Hilliard [33,34,75] and active-passive systems [74].

2. Laboratory and computer experiments on a model active system

Our experimental realization of two-dimensional dry active matter consists of brass rods of length 4.5 mm, with thickness tapered from 1.1 to 0.7 mm from tail to nose, and spherical aluminum

Downloaded from royalsocietypublishing.org/rsta/article-pdf/doi/10.1098/rsta.2025.0137/6175896/rsta.2025.0137.pdf
by Institue of Science & Technology Austria user
on 17 November 2026

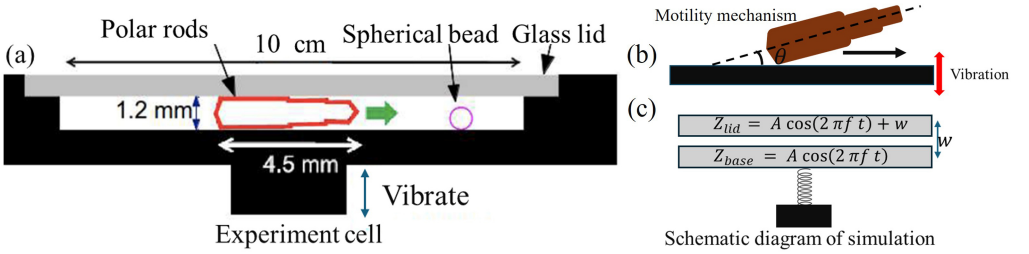


Figure 2. Schematic of the experimental and simulation set-ups. (a) Cross-section of the experimental cell. A mixture of polar, tapered rods (length 4.5 mm) and spherical beads is confined in a quasi-two-dimensional layer between a vertically vibrated base and a stationary glass lid, separated by a height of 1.2 mm. The vertical vibration provides the energy that the asymmetric shape of the rods transduces into directed, in-plane motion. (b) Cartoon depicting motility mechanism of an active polar particle. (c) Schematic of the corresponding simulation. The vibrating base and lid are modelled as two horizontal plates with vertical positions, Z_{base} and Z_{lid}, that oscillate sinusoidally with amplitude A and frequency f. The plates are maintained at a constant separation distance, w.

beads [13] of diameter 1 mm (figure 2a,b). The rod-bead mixture is confined between an anodized aluminium plate of diameter 12 cm and a glass lid, whose surfaces are separated by the distance w =1.2 mm. The plate is attached to a permanent magnetic shaker (LDS V406-PA100E), whose vertical agitation the rods transduce [24,66,76], by virtue of their shape and their dry friction against the bounding surfaces, into motion in the plane. All experiments are done at a shaker frequency $f = 200$ Hz and amplitude $A = 0.04$ mm, corresponding to a shaking strength $(2\pi f)^2 A = 7$ times the acceleration due to gravity. To observe the phenomenon in a quasi-one-dimensional setting, we create an annular geometry by gluing a circular block at the centre of the sample cell.

Our experiments are corroborated by numerical studies in a computer simulation which faithfully implements the mechanics of the experiment while offering the advantage of working with periodic boundary conditions (PBC) if desired, eliminating complications owing to boundaries in the plane. For numerical simplicity, we model each motile rod as an array of 13 overlapping beads with varying diameters chosen to best mimic the geometry of the experimental rods. The interaction of the particles with the sinusoidally oscillating plates is captured numerically through horizontal walls whose z-coordinates follow $Z_{\text{base}}(t) = A\cos(2\pi ft)$ and $Z_{\text{lid}}(t) = A\cos(2\pi ft) + w$ (figure 2c). The dynamics of the particles in the xy plane is restricted either to circular channels, as used in the experiments, or to a periodic square. The mass density ratio of the rods to the spherical beads is 3.3, corresponding to brass rods and aluminum beads. Consequently, the beads, being much lighter than the rods, can be easily pushed by them. All collisions occurring in the system—such as particle–particle and particle–wall collisions—are treated as instantaneous, inelastic interactions with contact friction, consistent with the experimental conditions. The impact of collisions between particles is implemented using a well-established rigid-body model from mechanical engineering, namely an impulse-based collision model [77]. The values of the friction and restitution coefficients for the various types of collisions (rod–rod, rod–bead, rod–base, rod–lid, bead–base, bead–lid, rod–wall and bead–wall) are chosen to ensure good agreement with the experimental observations.

An event-driven algorithm may seem a natural choice for simulating such hard-particle systems. However, the non-spherical shape of the rods makes this approach complicated and computationally expensive, as it requires solving complex transcendental equations to predict collisions. We therefore use a molecular dynamics algorithm to simulate the system. In addition, the rods in the experiments exhibit intrinsic noise owing to imperfect surface texture, which is absent in our simulations. This effect is incorporated by introducing an additional stochastic angular velocity ω_z to the rods about the z-direction. Whenever a rod collides with either of the horizontal walls, an additional angular velocity about the z-axis is imparted according to $\omega_z = \eta\,\epsilon\,v_z$, where η is a

Downloaded from royalsocietypublishing.org/rsta/article-pdf/doi/10.1098/rsta.2025.0137/6175896/rsta.2025.0137.pdf
by Institue of Science & Technology Austria user
on 17 November 2026

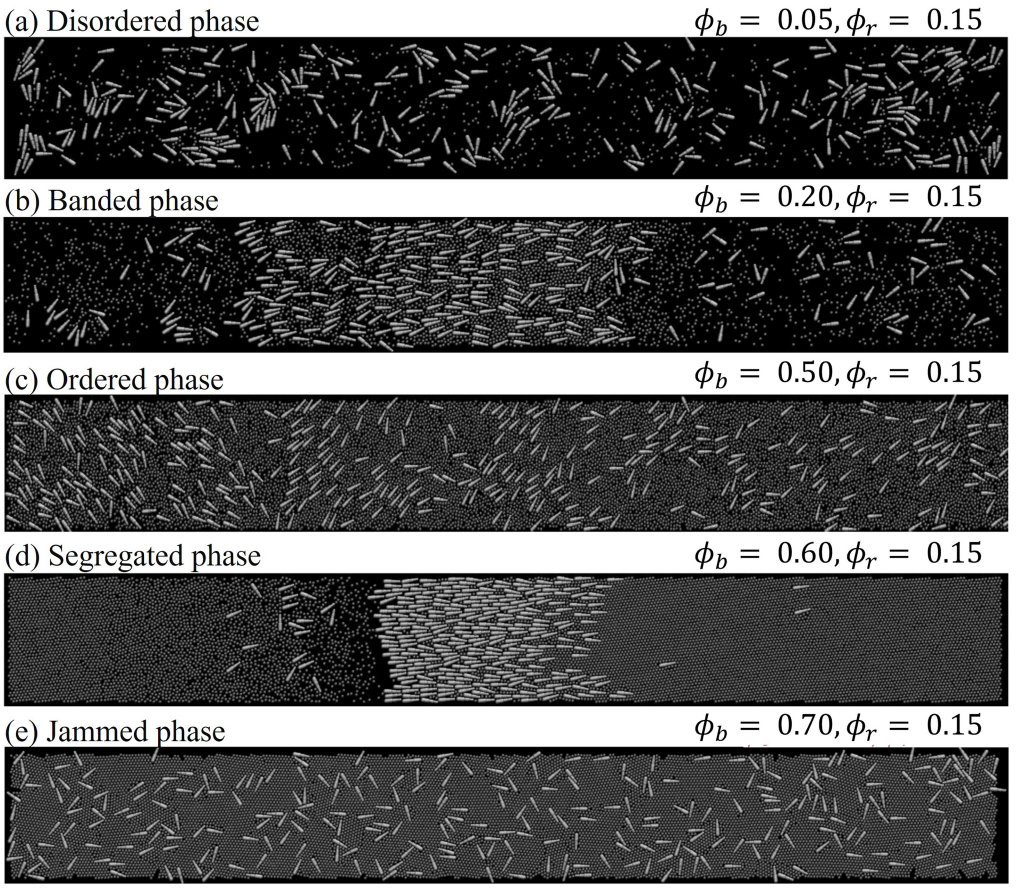


Figure 3. Different phases of rods and beads system in a channel geometry. (a) Disordered phase, rods move randomly in a disordered bead medium. (b) The banded phase, a thick band of rod-bead mixture in an isotropic state, moves together. (c) Ordered phase, in the homogeneous mixture of rods and beads, the rods flock along one particular direction. (d) Segregated phase, a homogeneous mixture of rods and beads, segregates into rods-rich and beads-rich regions and flock together. (e) Jammed phase, inert state of rods and beads. The dimensions of the simulation box along the long and short axes are 314*D* and 39*D*, respectively, where *D* is the bead diameter.

random variable taking values ±1 with equal probability, v_z is the relative contact velocity normal to the contact plane and ϵ is a fitting parameter.

3. Antidiffusivity and pattern formation

(a) Non-equilibrium phases: from flocking bands to complete segregation

Figure 3 shows the different states for a system of rods and beads in a channel geometry, at constant area fraction of rods $\phi_r = 0.15$ and varying area fraction of beads ϕ_b. These states are identical to those reported in [69], in a square box geometry. In particular, we are in the high-area-fraction regime, where the homogeneous mixture of rods and beads, at $\phi_r = 0.15$ and $\phi_b = 0.60$, phase-separates into rod-rich and bead-rich regions in the steady state (figure 3d). In this state, the whole system moves along the polar direction of the rods, that is, the narrow end forward, where a cluster of rods pushes the beads. This forcing owing to the rods leads to the formation of a high-density bead region in front of them.

The interesting thing about this transition is that the initial homogeneous, randomly ordered state of rods and beads first evolves to an ordered, uniform state of rods, that is, a homogeneous

Downloaded from royalsocietypublishing.org/rsta/article-pdf/doi/10.1098/rsta.2025.0137/6175896/rsta.2025.0137.pdf
by Institue of Science & Technology Austria user
on 17 November 2026

flock. In the steady state, the system settles into a segregated, ordered phase. This behaviour contrasts with the banded phase [69] (figure 3b), where bands form directly in the disordered state. Crystalline structures near the rods gradually melt into a gaseous structure further away (see [78] for details).

(b) The ultimate antidiffusive state: bulk condensation by an active interface

Having discussed flocking, banding and segregation in the previous section, here, the system exhibits its most profound antidiffusive behaviour, moving beyond simple segregation to achieve the macroscopic condensation of a passive fluid of hard spheres, driven by the collective action of a possibly sub-extensive active population. This section explores the ultimate state of self-organization, in which the active rods spontaneously form a one-dimensional active monolayer polarized along its normal. We will demonstrate how this emergent interfacial structure serves as the dynamic agent that organizes and compresses an extensive domain of beads. Finally, we will show how two such interfaces can cooperate to achieve 'active capture'—the complete immobilization and sequestration of a bulk passive cargo, providing a simple mechanical realization of the paradigmatic ability of a tiny active population to sculpt and control a vast passive environment (see [13] for the operation of such a mechanism for flocking rather than condensation).

(i) The core phenomenon: a self-assembled active membrane

The building block for the striking bulk condensation of passive particles that we now turn to is the spontaneous self-assembly of motile rods into a one-dimensional *active membrane* with a polarity along its normal. This process is observed in experiments within a quasi-one-dimensional annular channel, occurring at high bead density and low rod fraction (e.g. $\phi_b = 0.71$ and $\phi_r = 0.02$). Under these conditions, initially dispersed rods coalesce into a single, channel-spanning polar monolayer, both lying at and creating the sharp interface between bead-rich and bead-poor domains (figure 4a). Structurally, this object consists of rods aligned side-by-side, with their tapered tips pointing uniformly in the azimuthal direction, giving it a coherent and persistent motility. This entire phenomenon from the initial coalescence to the formation of a stable, polarized interface is robustly reproduced in mechanically detailed simulations (figure 4d), confirming it as the central organizational motif of the system.

(ii) Active capture and immobilization: a mechanism for cargo sequestration

Increasing the rod fraction in the quasi-one-dimensional annular geometry to $\phi_r \approx 0.04 - 0.05$ leads to the formation of two separate active membranes. These membranes are oppositely polarized and consequently sequester the bulk domain of passive beads between them (figure 4b,c). Initially, the opposing interfaces act as motile (and mobile) active interfaces, moving towards each other and shrinking the entrapped bead-rich region. A stable, steady state is reached when the compressive pressure exerted by the condensed beads balances the force of the rods, which arrests all large-scale motion. The final state consists of an immobile, highly ordered crystalline domain of beads permanently trapped between the two active interfaces.

We term this phenomenon **active capture**, as it provides a direct mechanical analogue for cargo sequestration. The stability of this captured state is maintained by a self-sorting mechanism. Any imbalance in the propulsive forces between the two interfaces would cause a net drift of the entire structure. This motion, in turn, liberates rods from the trailing edge, whence they defect and are captured by the leading edge. This process equalizes the rod populations at the interfaces, balances the opposing forces and restores the globally immobile state.

Downloaded from royalsocietypublishing.org/rsta/article-pdf/doi/10.1098/rsta.2025.0137/6175896/rsta.2025.0137.pdf
by Institue of Science & Technology Austria user
on 17 November 2026

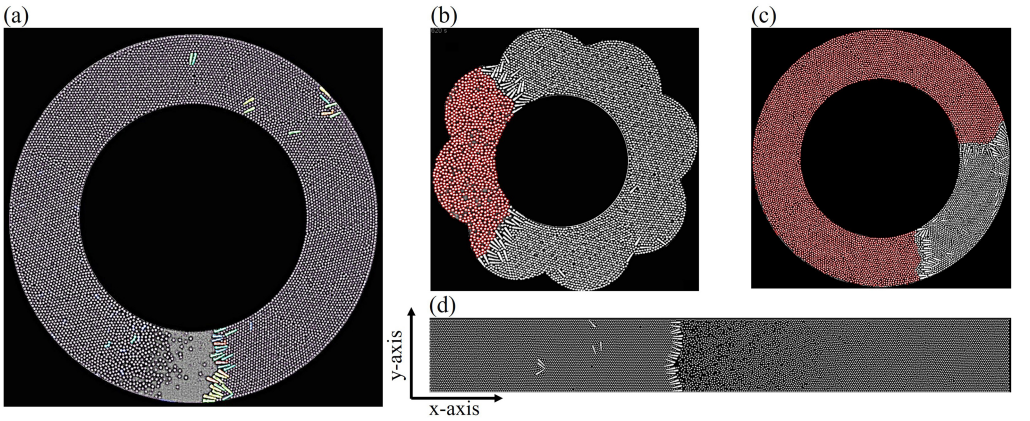


Figure 4. Bulk condensation and active capture by self-assembled monolayers in quasi-one-dimensional geometries. (a) Experimental observation of bulk condensation in an annular channel. A single polar monolayer of active rods ($\phi_r = 0.02$ and $\phi_b = 0.71$) forms a coherent interface that condenses a macroscopic domain of passive beads. (b and c) Snapshots showing active capture by two opposing monolayers, which trap an immobile, crystalline domain of beads. This is shown for a geometry with a smooth outer boundary in panel (c), where $\phi_b = 0.70$, $\phi_r = 0.05$ and the inner block radius is 2.5 cm, and for a floral outer boundary in panel (b), where $\phi_b = 0.71$, $\phi_r = 0.04$ and the inner block radius is 4 cm. (d) The same condensation phenomenon is realized in simulations within a straight channel ($249D \times 31D$) with PBC, demonstrating that the mechanism is not dependent on the curved geometry ($\phi_b = 0.75$ and $\phi_r = 0.015$). Images from [73].

(iii) Condensing a bulk passive domain in quasi-two dimensions

Having established the key features of condensation within the quasi-one-dimensional geometry, we now explore the two-dimensional phase diagram to determine whether similar transitions and structures emerge in higher dimensions. For rod area fraction $\phi_r = 0$, the system displays fluid, hexatic and crystalline phases as a function of bead area fraction ϕ_b [79].

The experimental phase diagram in the ϕ_b–ϕ_r plane, shown in figure 5, reveals this rich progression of states. For a two-dimensional system at a low rod fraction of $\phi_r = 0.06$, increasing the bead fraction drives the system through a sequence of distinct phases. At low bead density ($\phi_b = 0.55$), the system is in a homogeneous isotropic state, with particles distributed randomly and showing no organized motion. Crossing a first threshold ($\phi_b = 0.70$) induces a transition to a homogeneous flock, where polar-rod orientations and all particle velocities align along a common azimuthal direction, as previously reported in [13]. Past a second threshold ($\phi_b = 0.72$), the system exhibits clear rod-bead segregation.

The third and most striking transition occurs as ϕ_b is further increased. For the representative case of $\phi_r = 0.06$, the threshold value $\phi_b = 0.77$ marks the onset of the self-assembled polar monolayer, which in turn condenses a bulk domain of beads (figure 5). In this state, the rods align side by side, with their tapered tips pointing towards the dense, immobile bead region. The onset of this active self-assembly occurs along a locus in the phase diagram defined by $\phi_r + \phi_b \approx 0.83$. The resulting bead domains on either side of the monolayer differ distinctly: while the packing fraction changes only slightly, their mobility varies considerably [73]. Numerical simulations confirm the robustness of this interfacial condensation across different conditions. In square domains with PBC, coherently moving one-dimensional polar membranes readily form at high bead and low rod fractions (e.g. $\phi_b = 0.80$ and $\phi_r = 0.03$), as seen in figure 5c. Crucially, the phenomenon is not an artefact of the boundary conditions, as simulations in rectangular domains *without* PBC also exhibit stable coexistence between high- and low-density bead regions.

The single-rod motility, u_0, is a key control parameter for the nature of this phase separation. Tuning this parameter reveals a distinct motility threshold below which condensation is absent. Above this threshold, increasing u_0 transforms the density profile at the active interface from a

Downloaded from royalsocietypublishing.org/rsta/article-pdf/doi/10.1098/rsta.2025.0137/6175896/rsta.2025.0137.pdf
by Institue of Science & Technology Austria user
on 17 November 2026

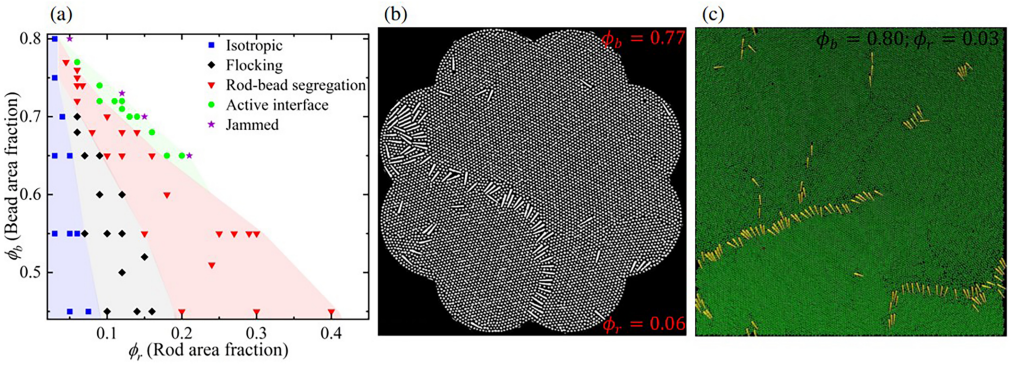


Figure 5. The progression to bulk condensation in two dimensions: phase diagram and representative states. (a) The experimental phase diagram in the ϕ_b–ϕ_r plane. With increasing bead density, the system transitions from an isotropic gas to a homogeneous flock to rod-bead segregation and finally to the state of primary interest: condensation by a self-assembled active interface. The 'jammed' state denotes a regime of extreme packing (total area fraction $\simeq 0.85$) where particle dynamics are nearly arrested. (b) An experimental snapshot illustrating the bulk condensation state. A self-assembled monolayer of aligned rods ($\phi_b = 0.77$ and $\phi_r = 0.06$) is seen actively condensing the dense domain of beads. (c) A corresponding simulation of a travelling active interface in a square box (length 249 bead diameters) with PBC, confirming the robustness of the phenomenon ($\phi_b = 0.80$ and $\phi_r = 0.03$). Images from [73].

smooth gradient into a sharp, shock-like front. Experiments and simulations demonstrate that even a small fraction of active rods can condense a bulk domain of passive beads (see [73] for details).

4. Theoretical framework: a hydrodynamic theory of active segregation

In this section, we first describe the intuitive physical mechanism behind this instability and then briefly outline the coarse-grained hydrodynamic theory that formalizes it. The origin of segregation is a self-amplifying feedback driven by active forcing and particle shape. The mechanism unfolds in two steps. First, a group of coherently moving rods imparts active forcing on the passive beads, pushing them forward and creating a local bead-density gradient. Second, the tapered, asymmetric shape of the rods creates a strong steric preference for them to align *up* this gradient, with their narrow ends pointing into the denser region. This enhanced alignment, in turn, increases the magnitude of the collective active forcing on the bead medium, thereby steepening the density gradient. This instability drives an initially homogeneous mixture towards the observed condensed state, assisted by an active membrane.

(a) Dynamical equations

We now show that the mechanism and broad features of the demixing of active rods and passive beads can be understood within a coarse-grained theory. The hydrodynamic fields in our description are the number densities ρ and σ of beads and rods. We denote $\mathbf{P}$ as the local average of the unit vectors of individual rods, defined to point from the broad tail to the narrow nose, which is also the direction in which they self-propel. We ignore the interplay [13,80] of rod orientation with the hydrodynamic flow of beads, which, if included, only leads to finite shifts of thresholds. The conservation of beads and rods is expressed in the continuity equations

$$\partial_t \rho + \nabla \cdot \mathbf{J}_\rho = 0 \text{ and } \partial_t \sigma + \nabla \cdot \mathbf{J}_\sigma = 0 \tag{4.1}$$

Downloaded from royalsocietypublishing.org/rsta/article-pdf/doi/10.1098/rsta.2025.0137/6175896/rsta.2025.0137.pdf
by Institue of Science & Technology Austria user
on 17 November 2026

with currents

$$\begin{aligned}\mathbf{J}_\rho &= -M_\rho \nabla \delta F/\delta\rho + \alpha\rho\mathbf{P} \\ &\simeq -D_\rho \nabla\rho - M_\rho w \nabla\sigma + \alpha\rho\mathbf{P} \end{aligned} \tag{4.2}$$

$$\begin{aligned}\text{and } \mathbf{J}_\sigma &= -M_\sigma \nabla \delta F/\delta\sigma + u_0\sigma\mathbf{P} \\ &\simeq -D_\sigma \nabla\sigma - M_\sigma w \nabla\rho + u_0\sigma\mathbf{P}. \end{aligned} \tag{4.3}$$

While our system is not thermal, equations (4.2) and (4.3) assume a reference equilibrium-like passive dynamics with a diagonal mobility matrix diag(M_ρ, M_σ). This is simply to have a reference equilibrium system as a point of departure. An interaction term $w\rho\sigma$ in the free-energy functional F introduces cross-couplings, resulting in direct and cross diffusive fluxes in equations (4.2) and (4.3). For hard particles, $w > 0$ represents excluded volume. Given that $D_\rho, D_\sigma > 0$, we are not in a regime where either species condenses independently. Activity enters through $u_0 > 0$ and α, which, respectively, set the scales of rod motility and forcing of bead motion by the rods, along $\mathbf{P}$ [13]. We work directly with averaged, that is, non-stochastic, quantities, but allow for spatial inhomogeneity. To close the equation, we must have a dynamical equation for $\mathbf{P}$, which is an extension of [13], [25] and [26]. For the isotropic phase, $\mathbf{P}$ relaxes rapidly compared to the slow evolution of the densities and anchors to the local density gradient $(a - K\nabla^2)\mathbf{P} = A\nabla\rho + B\nabla\sigma$, with phenomenological couplings a, (A, B) and elastic stiffness constant K (see [73] for a more detailed discussion). Linearizing and expanding up to second order in gradients, we see that

$$\mathbf{P} \simeq \frac{1}{a}(A\nabla\rho + B\nabla\sigma) + \frac{K}{a^2}\nabla^2(A\nabla\rho + B\nabla\sigma). \tag{4.4}$$

The essence of the antidiffusive instability reveals itself when we substitute equation (4.4) back into the equations for density currents to perform linear stability analysis around uniform mixtures ρ_0 and σ_0, which, defining $D_{\rho\sigma} = wM_\rho$ and $D_{\sigma\rho} = wM_\sigma$, yields,

$$\partial_t\delta\rho = \left[\left(D_\rho - \frac{\rho_0\alpha A}{a}\right)\nabla^2 - \frac{\rho_0\alpha AK}{a^2}\nabla^4\right]\delta\rho + \left[\left(D_{\rho\sigma} - \frac{\rho_0\alpha B}{a}\right)\nabla^2 - \frac{\rho_0\alpha BK}{a^2}\nabla^4\right]\delta\sigma \tag{4.5}$$

$$\text{and } \partial_t\delta\sigma = \left[\left(D_{\sigma\rho} - \frac{\sigma_0 u_0 A}{a}\right)\nabla^2 - \frac{\sigma_0 u_0 AK}{a^2}\nabla^4\right]\delta\rho + \left[\left(D_\sigma - \frac{\sigma_0 u_0 B}{a}\right)\nabla^2 - \frac{\sigma_0 u_0 BK}{a^2}\nabla^4\right]\delta\sigma. \tag{4.6}$$

The positive active terms $\frac{\rho_0\alpha A}{a}$ and $\frac{\sigma_0 u_0 B}{a}$ act in direct opposition to stabilizing bare diffusivity D_ρ and D_σ from passive dynamics. The physical mechanism described at the beginning of the section guarantees that $\alpha A > 0$: sterically, a rod's narrow nose penetrates dense bead regions more easily than its broad tail, biasing rods to point up bead-density gradients ($A > 0$); simultaneously, rods pushing beads forward generate density gradients along their polarization axis ($\alpha > 0$). When these activity and polarity parameters are sufficiently large, the effective diffusion coefficients become negative. This change in sign marks the onset of a classic spinodal decomposition, the definitive signature of antidiffusion causing macroscopic phase separation. Note that in equations (4.5) and (4.6) both antidiffusion and the stabilizing ∇^4 terms are proportional to the activity parameters α and u_0. There is a curious and not fully understood (by us, at least) parallel here to the Cahn–Hilliard equation [3], where both the corresponding terms again have a single origin in microscopic theory, namely, an attractive interaction. Moreover, the presence of active contributions proportional to α and u_0 can lead to opposite signs for the off-diagonal couplings in equations (4.5) and (4.6), and therefore to *non-reciprocal* Cahn–Hilliard dynamics [33,34].

Downloaded from royalsocietypublishing.org/rsta/article-pdf/doi/10.1098/rsta.2025.0137/6175896/rsta.2025.0137.pdf
by Institue of Science & Technology Austria user
on 17 November 2026

5. Discussion, outlook and future prospects

In this article, we have shown that antidiffusion occurs widely in active matter. In suspensions of swimming particles, antidiffusive instabilities arise through feedback between flow created by swimmers and reorganization of swimmers by flow, with the appearance of negative diffusivities of orientation, velocity [48] and concentration [49] depending on the case at hand. Distinct classes of antidiffusive instability arise in viscous [44–46] and inertial [48,49] settings, and in regimes dominated by the motility of the particles or by the force dipoles they carry. In 'dry' active systems, that is, particles moving on or through an inert momentum sink such as a solid substrate, the important interplay is between persistent motility and excluded volume, though effects resembling a hydrodynamic interaction enter if the active particles move amidst a bath of passive diffusing particles [13,73].

Although we discussed bulk active fluids in the introduction, our focus in this article has been on a dry system consisting of motile rods of polar, that is, fore-aft asymmetric, shape and spherical beads whose motion is diffusive. We have shown that a phenomenon resembling condensation—more properly sublimation, as the condensed phase is crystalline—arises from the sequestering effect of the polar rods on the beads. While the diverse mechanisms of active antidiffusion surveyed earlier—whether driven by autochemotaxis [57], crowding [55] or torques [54]—typically describe the phase separation of the active species itself, in our system a dilute active minority self-assembles into a polar membrane that acts as the agent to condense a bulk passive medium.

Our linearized theory of this phenomenon finds an instability governed by a negative effective diffusivity, i.e. spinodal decomposition, which can be regarded as the limit of metastability of the homogeneous phase. Our experiments never display the modulations in the bead density that one would associate with this kinetic pathway. Instead, the polar rods seek and find one another from afar—possibly a kind of nucleation—and rapidly self-assemble into a single row, which constitutes the interface between the high and low bead densities they create ahead and astern of themselves. It should be possible to extend the framework of Active Model B+ [58,81], the scalar field theory for phase separation in active systems with a conserved order parameter, to provide a theory of coexistence between dense and dilute passive regions taking into account the role of the orientable and motile species at the interface, possibly in the form of an 'uncommon tangents' construction [20]. This is not a typical antidiffusion issue, but it is a problem of central interest if one aims to build a steady-state thermodynamics of active matter. The contrasts between our study of active-passive mixtures and that of [50] are interesting. Their core-halo phase separation is transient; ours appears to be permanent. Their condensed structures are finite; ours are practically unbounded in the direction of motion. It seems clear that the difference originates in the active-particle shape. Our motile species consists of elongated particles with fore-aft asymmetric structure, whereas Stenhammar *et al.* [50] consider discs. Active-particle shape is therefore an important and multi-dimensional 'knob' to be exploited in active self-assembly. A natural extension of the active-rod/passive-bead system would be to consider two species that are unequally dragged by the motion of the polar rods. The resulting phase separation, for which it should be possible to build a coarse-grained theory, would allow one to make a connection to problems of segregation of motor species in microtubule motility assays [82]. Such a field theory would involve aspects of Active Model B+ [58,81], non-reciprocal Cahn–Hilliard physics [33,34], and active-passive mixtures [17,50,74,83], complicated by the presence of three components.

Unifying connections among the diverse examples of antidiffusion we have summarized, and especially between those in active matter and in other settings, remain to be explored. In particular, our discussion in this article is entirely on instabilities of a homogeneous reference state. The possible emergence of structures such as staircases through instabilities about a reference state with a mean gradient, as discussed for large-scale flows [38], and the differences in this regard between 'wet' and 'dry' systems are subjects that merit further study.

Downloaded from royalsocietypublishing.org/rsta/article-pdf/doi/10.1098/rsta.2025.0137/6175896/rsta.2025.0137.pdf
by Institue of Science & Technology Austria user
on 17 November 2026

Data accessibility. All images in the figure including those based on computer simulation data are from published work, duly cited in the paper. They are presented as qualitative illustrations and not for conveying quantitative information.

Declaration of AI use. We have not used AI-assisted technologies in creating this article.

Authors' contributions. R.K.: conceptualization, formal analysis, investigation, methodology, visualization, writing—original draft, writing—review and editing; H.S.: conceptualization, formal analysis, investigation, methodology, software, visualization, writing—original draft, writing—review and editing; R.K.G.: conceptualization, investigation, software, writing—original draft, writing—review and editing; A.K.S.: conceptualization, investigation, methodology, writing—original draft, writing—review and editing; S.R.: conceptualization, formal analysis, funding acquisition, investigation, methodology, supervision, writing—original draft, writing—review and editing.

All authors gave final approval for publication and agreed to be held accountable for the work performed therein.

Conflict of interest declaration. We declare we have no competing interests.

Funding. S.R. acknowledges support from the ANRF India through a National Science Chair, grant SP/ANRF-24-0081, and a J. C. Bose Fellowship, and an Endowed Visiting Professorship from ICTS-TIFR. R.K. was supported by the UGC and the ANRF, India; A.K.S. acknowledges a National Science Chair Professorship of the ANRF, India, and H.S. thanks the ANRF, India, for support under grant SRG/2022/000061-G. S.R. thanks the Isaac Newton Institute for Mathematical Sciences, Cambridge, for a Rothschild Distinguished Visiting Fellowship and for support and hospitality during the programme Anti-diffusive dynamics: from subcellular to astrophysical scales, supported by EPSRC grant no. EP/R014604/1.

Acknowledgements. We thank M Barma, ME Cates, A Maitra, R Mondal, C Nardini and M Rao for illuminating discussions.

References

1. Cross MC, Hohenberg PC. 1993 Pattern formation outside of equilibrium. *Rev. Mod. Phys.* **65**, 851–1112. (doi:10.1103/RevModPhys.65.851)
2. Cahn JW, Hilliard JE. 1958 Free energy of a nonuniform system. I. Interfacial free energy. *J. Chem. Phys.* **28**, 258–267. (doi:10.1063/1.1744102)
3. Cahn JW. 1965 Phase separation by spinodal decomposition in isotropic systems. *J. Chem. Phys.* **42**, 93–99. (doi:10.1063/1.1695731)
4. Toner J, Tu Y, Ramaswamy S. 2005 Hydrodynamics and phases of flocks. *Ann. Phys.* **318**, 170–244. (doi:10.1016/j.aop.2005.04.011)
5. Ramaswamy S. 2017 Active matter. *J. Stat. Mech. Theory Exp.* **2017**, 054002. (doi:10.1088/1742-5468/aa6bc5)
6. Ramaswamy S. 2010 The mechanics and statistics of active matter. *Annu. Rev. Condens. Matter Phys.* **1**, 323–345. (doi:10.1146/annurev-conmatphys-070909-104101)
7. Prost J, Jülicher F, Joanny JF. 2015 Active gel physics. *Nat. Phys.* **11**, 111–117. (doi:10.1038/nphys3224)
8. Marchetti MC, Joanny JF, Ramaswamy S, Liverpool TB, Prost J, Rao M, Simha RA. 2013 Hydrodynamics of soft active matter. *Rev. Mod. Phys.* **85**, 1143–1189. (doi:10.1103/RevModPhys.85.1143)
9. Shankar S, Souslov A, Bowick MJ, Marchetti MC, Vitelli V. 2022 Topological active matter. *Nat. Rev. Phys.* **4**, 380–398. (doi:10.1038/s42254-022-00445-3)
10. Chaté H. 2020 Dry aligning dilute active matter. *Annu. Rev. Condens. Matter Phys.* **11**, 189–212. (doi:10.1146/annurev-conmatphys-031119-050752)
11. Bowick MJ, Fakhri N, Marchetti MC, Ramaswamy S. 2022 Symmetry, thermodynamics, and topology in active matter. *Phys. Rev. X* **12**, 010501. (doi:10.1103/PhysRevX.12.010501)
12. Bechinger C, Di Leonardo R, Löwen H, Reichhardt C, Volpe G, Volpe G. 2016 Active particles in complex and crowded environments. *Rev. Mod. Phys.* **88**, 045006. (doi:10.1103/RevModPhys.88.045006)
13. Kumar N, Soni H, Ramaswamy S, Sood A. 2014 Flocking at a distance in active granular matter. *Nat. Commun.* **5**, 4688. (doi:10.1038/ncomms5688)
14. Bell S, Ackermann J, Maitra A, Voituriez R. 2025 Ordering spontaneous flows and aging in active fluids depositing tracks. *Phys. Rev. E* **111**, L023405. (doi:10.1103/PhysRevE.111.L023405)

Downloaded from royalsocietypublishing.org/rsta/article-pdf/doi/10.1098/rsta.2025.0137/6175896/rsta.2025.0137.pdf
by Institue of Science & Technology Austria user
on 17 November 2026

15. Ganai N, Sengupta S, Menon GI. 2014 Chromosome positioning from activity-based segregation. *Nucleic Acids Res.* **42**, 4145–4159. (doi:10.1093/nar/gkt1417)
16. Weber SN, Weber CA, Frey E. 2016 Binary mixtures of particles with different diffusivities demix. *Phys. Rev. Lett.* **116**, 058301. (doi:10.1103/PhysRevLett.116.058301)
17. Grosberg AY, Joanny JF. 2015 Nonequilibrium statistical mechanics of mixtures of particles in contact with different thermostats. *Phys. Rev. E* **92**, 032118. (doi:10.1103/PhysRevE.92.032118)
18. Riedel IH, Kruse K, Howard J. 2005 A self-organized vortex array of hydrodynamically entrained sperm cells. *Science* **309**, 300–303. (doi:10.1126/science.1110329)
19. Sumino Y, Nagai K, Shitaka Y, Tanaka D, Yoshikawa K, Chaté H, Oiwa K. 2012 Large-scale vortex lattice emerging from collectively moving microtubules. *Nature* **483**, 448–452. (doi:10.1038/nature10874)
20. Cates ME, Tailleur J. 2015 Motility-induced phase separation. *Annu. Rev. Condens. Matter Phys.* **6**, 219–244. (doi:10.1146/annurev-conmatphys-031214-014710)
21. Thampi SP, Doostmohammadi A, Golestanian R, Yeomans JM. 2015 Intrinsic free energy in active nematics. *Europhys. Lett.* **112**, 28004. (doi:10.1209/0295-5075/112/28004)
22. Shankar S, Ramaswamy S, Marchetti MC, Bowick MJ. 2018 Defect unbinding in active nematics. *Phys. Rev. Lett.* **121**, 108002. (doi:10.1103/PhysRevLett.121.108002)
23. Romanczuk P, Chaté H, Chen L, Ngo S, Toner J. 2016 Emergent smectic order in simple active particle models. *New J. Phys.* **18**, 063015. (doi:10.1088/1367-2630/18/6/063015)
24. Narayan V, Ramaswamy S, Menon N. 2007 Long-lived giant number fluctuations in a swarming granular nematic. *Science* **317**, 105–108. (doi:10.1126/science.1140414)
25. Toner J, Tu Y. 1995 Long-range order in a two-dimensional dynamical XY model: how birds fly together. *Phys. Rev. Lett.* **75**, 4326–4329. (doi:10.1103/PhysRevLett.75.4326)
26. Toner J, Tu Y. 1998 Flocks, herds, and schools: a quantitative theory of flocking. *Phys. Rev. E* **58**, 4828–4858. (doi:10.1103/PhysRevE.58.4828)
27. Maitra A. 2023 Two-dimensional long-range uniaxial order in three-dimensional active fluids. *Nat. Phys.* **19**, 733–740. (doi:10.1038/s41567-023-01937-4)
28. Banerjee D, Souslov A, Abanov A, Vitelli V. 2017 Odd viscosity in chiral active fluids. *Nat. Commun.* **8**, 1573. (doi:10.1038/s41467-017-01378-7)
29. Tan TH, Mietke A, Li J, Chen Y, Higinbotham H, Foster PJ, Gokhale S, Dunkel J, Fakhri N. 2022 Odd dynamics of living chiral crystals. *Nature* **607**, 287–293. (doi:10.1038/s41586-022-04889-6)
30. Avron JE. 1998 Odd viscosity. *J. Stat. Phys.* **92**, 543–557. (doi:10.1023/A:1023084404080)
31. Scheibner C, Souslov A, Banerjee D, Surówka P, Irvine WTM, Vitelli V. 2020 Odd elasticity. *Nat. Phys.* **16**, 475–480. (doi:10.1038/s41567-020-0795-y)
32. Fruchart M, Hanai R, Littlewood PB, Vitelli V. 2021 Non-reciprocal phase transitions. *Nature* **592**, 363–369. (doi:10.1038/s41586-021-03375-9)
33. You Z, Baskaran A, Marchetti MC. 2020 Nonreciprocity as a generic route to traveling states. *Proc. Natl Acad. Sci. USA* **117**, 19 767–19 772. (doi:10.1073/pnas.2010318117)
34. Saha S, Agudo-Canalejo J, Golestanian R. 2020 Scalar active mixtures: the nonreciprocal Cahn–Hilliard model. *Phys. Rev. X* **10**, 041009. (doi:10.1103/PhysRevX.10.041009)
35. Aditi Simha R, Ramaswamy S. 2002 Hydrodynamic fluctuations and instabilities in ordered suspensions of self-propelled particles. *Phys. Rev. Lett.* **89**, 058101. (doi:10.1103/PhysRevLett.89.058101)
36. Voituriez R, Joanny JF, Prost J. 2005 Spontaneous flow transition in active polar gels. *Europhys. Lett.* **70**, 404–410. (doi:10.1209/epl/i2004-10501-2)
37. Alert R, Casademunt J, Joanny JF. 2022 Active turbulence. *Annu. Rev. Condens. Matter Phys.* **13**, 143–170. (doi:10.1146/annurev-conmatphys-082321-035957)
38. Ramirez F, Diamond P. 2025 Staircases of passive and active scalar concentration in cellular flow. *Phys. Plasmas* **32**, 072302. (doi:10.1063/5.0260948)
39. Dif-Pradalier G *et al*. 2015 Finding the elusive $\mathbf{E} \times \mathbf{B}$ staircase in magnetized plasmas. *Phys. Rev. Lett.* **114**, 085004. (doi:10.1103/PhysRevLett.114.085004)
40. Pružina P, Hughes DW, Pegler SS. 2022 Development and long-term evolution of density staircases in stirred stratified turbulence. *Phys. Rev. Fluids* **7**, 104801. (doi:10.1103/PhysRevFluids.7.104801)
41. Brennen C, Winet H. 1977 Fluid mechanics of propulsion by cilia and flagella. *Annu. Rev. Fluid Mech.* **9**, 339–398. (doi:10.1146/annurev.fl.09.010177.002011)

Downloaded from royalsocietypublishing.org/rsta/article-pdf/doi/10.1098/rsta.2025.0137/6175896/rsta.2025.0137.pdf
by Institue of Science & Technology Austria user
on 17 November 2026

42. Ramaswamy S, Rao M. 2007 Active-filament hydrodynamics: instabilities, boundary conditions and rheology. *New J. Phys.* **9**, 423. (doi:10.1088/1367-2630/9/11/423)
43. Maitra A, Srivastava P, Marchetti MC, Lintuvuori JS, Ramaswamy S, Lenz M. 2018 A nonequilibrium force can stabilize 2D active nematics. *Proc. Natl Acad. Sci. USA* **115**, 6934–6939. (doi:10.1073/pnas.1720607115)
44. Hatwalne Y, Ramaswamy S, Rao M, Simha RA. 2004 Rheology of active-particle suspensions. *Phys. Rev. Lett.* **92**, 118101. (doi:10.1103/PhysRevLett.92.118101)
45. López HM, Gachelin J, Douarche C, Auradou H, Clément E. 2015 Turning bacteria suspensions into superfluids. *Phys. Rev. Lett.* **115**, 028301. (doi:10.1103/PhysRevLett.115.028301)
46. Marchetti MC. 2015 Frictionless fluids from bacterial teamwork. *Nature* **525**, 37–39. (doi:10.1038/525037a)
47. Dadhichi LP, Sahoo SK, Kumar KV, Ramaswamy S. 2026 Superdiffusion and antidiffusion in an aligned active suspension. *Phys. Rev. Lett.* **136**, 128302. (doi:10.1103/d61l-1tyh)
48. Chatterjee R, Rana N, Simha RA, Perlekar P, Ramaswamy S. 2021 Inertia drives a flocking phase transition in viscous active fluids. *Phys. Rev. X* **11**, 031063. (doi:10.1103/PhysRevX.11.031063)
49. Jain P, Rana N, Ramaswamy S, Perlekar P. 2024 Inertia drives concentration-wave turbulence in swimmer suspensions. *Phys. Rev. Lett.* **133**, 158302. (doi:10.1103/PhysRevLett.133.158302)
50. Stenhammar J, Wittkowski R, Marenduzzo D, Cates ME. 2015 Activity-induced phase separation and self-assembly in mixtures of active and passive particles. *Phys. Rev. Lett.* **114**, 018301. (doi:10.1103/PhysRevLett.114.018301)
51. Chajwa R, Rajarshi C, Govindarajan R, Ramaswamy S. 2026 Active caustics. *Phys. Rev. Fluids* **11**, 033104. (doi:10.1103/m3v2-bdvj)
52. Keller EF, Segel LA. 1970 Initiation of slime mold aggregation viewed as an instability. *J. Theor. Biol.* **26**, 399–415. (doi:10.1016/0022-5193(70)90092-5)
53. Palacci J, Sacanna S, Steinberg AP, Pine DJ, Chaikin PM. 2013 Living crystals of light-activated colloidal surfers. *Science* **339**, 936–940. (doi:10.1126/science.1230020)
54. Zhang J, Alert R, Yan J, Wingreen NS, Granick S. 2021 Active phase separation by turning towards regions of higher density. *Nat. Phys.* **17**, 961–967. (doi:10.1038/s41567-021-01238-8)
55. Geyer D, Martin D, Tailleur J, Bartolo D. 2019 Freezing a flock: motility-induced phase separation in polar active liquids. *Phys. Rev. X* **9**, 031043. (doi:10.1103/PhysRevX.9.031043)
56. Wilkinson M, Mehlig B. 2005 Caustics in turbulent aerosols. *Europhys. Lett.* **71**, 186–192. (doi:10.1209/epl/i2004-10532-7)
57. Miller M, Toner J. 2024 Following your nose: autochemotaxis and other mechanisms for spinodal decomposition in flocks. *Phys. Rev. Lett.* **132**, 128301. (doi:10.1103/PhysRevLett.132.128301)
58. Cates ME, Nardini C. 2025 Active phase separation: new phenomenology from nonequilibrium physics. *Rep. Prog. Phys.* **88**, 056601. (doi:10.1088/1361-6633/add278)
59. Fily Y, Marchetti MC. 2012 Athermal phase separation of self-propelled particles with no alignment. *Phys. Rev. Lett.* **108**, 235702. (doi:10.1103/PhysRevLett.108.235702)
60. Tailleur J, Cates ME. 2008 Statistical mechanics of interacting run-and-tumble bacteria. *Phys. Rev. Lett.* **100**, 218103. (doi:10.1103/PhysRevLett.100.218103)
61. Redner GS, Hagan MF, Baskaran A. 2013 Structure and dynamics of a phase-separating active colloidal fluid. *Phys. Rev. Lett.* **110**, 055701. (doi:10.1103/PhysRevLett.110.055701)
62. Bricard A, Caussin JB, Desreumaux N, Dauchot O, Bartolo D. 2013 Emergence of macroscopic directed motion in populations of motile colloids. *Nature* **503**, 95–98. (doi:10.1038/nature12673)
63. Mishra S, Puri S, Ramaswamy S. 2014 Aspects of the density field in an active nematic. *Phil. Trans. R. Soc. A* **372**, 20130364. (doi:10.1098/rsta.2013.0364)
64. Ramaswamy S, Simha RA, Toner J. 2003 Active nematics on a substrate: giant number fluctuations and long-time tails. *EPL* **62**, 196. (doi:10.1209/epl/i2003-00346-7)
65. Sharma A, Soni H. 2024 Phases and correlations in active nematic granular systems. *Soft Matter* **20**, 6608–6617. (doi:10.1039/D4SM00667D)
66. Yamada D, Hondou T, Sano M. 2003 Coherent dynamics of an asymmetric particle in a vertically vibrating bed. *Phys. Rev. E* **67**, 040301. (doi:10.1103/PhysRevE.67.040301)
67. Narayan V. 2010 Phase behaviour and dynamics of an agitated monolayer of granular rods. PhD thesis, Indian Institute of Science, India.

Downloaded from royalsocietypublishing.org/rsta/article-pdf/doi/10.1098/rsta.2025.0137/6175896/rsta.2025.0137.pdf
by Institue of Science & Technology Austria user
on 17 November 2026

68. Kumar N. 2015 Driven granular and soft-matter: fluctuation relations, cooperative motion and oscillatory sedimentation. PhD thesis, Indian Institute of Science, India.
69. Soni H, Kumar N, Nambisan J, Gupta RK, Sood AK, Ramaswamy S. 2020 Phases and excitations of active rod–bead mixtures: simulations and experiments. *Soft Matter* **16**, 7210–7221. (doi:10.1039/C9SM02552A)
70. Deseigne J, Dauchot O, Chaté H. 2010 Collective motion of vibrated polar disks. *Phys. Rev. Lett.* **105**, 098001. (doi:10.1103/PhysRevLett.105.098001)
71. Weber CA, Hanke T, Deseigne J, Léonard S, Dauchot O, Frey E, Chaté H. 2013 Long-range ordering of vibrated polar disks. *Phys. Rev. Lett.* **110**, 208001. (doi:10.1103/PhysRevLett.110.208001)
72. Clewett JP, Roeller K, Bowley RM, Herminghaus S, Swift MR. 2012 Emergent surface tension in vibrated, noncohesive granular media. *Phys. Rev. Lett.* **109**, 228002. (doi:10.1103/PhysRevLett.109.228002)
73. Kant R, Gupta RK, Soni H, Sood AK, Ramaswamy S. 2024 Bulk condensation by an active interface. *Phys. Rev. Lett.* **133**, 208301. (doi:10.1103/PhysRevLett.133.208301)
74. Wittkowski R, Stenhammar J, Cates ME. 2017 Nonequilibrium dynamics of mixtures of active and passive colloidal particles. *New J. Phys.* **19**, 105003. (doi:10.1088/1367-2630/aa8195)
75. Saha S. 2024 Phase coexistence in the non-reciprocal Cahn–Hilliard model. (doi:10.48550/arXiv.2402.10057)
76. Kudrolli A, Lumay G, Volfson D, Tsimring LS. 2008 Swarming and swirling in self-propelled polar granular rods. *Phys. Rev. Lett.* **100**, 058001. (doi:10.1103/PhysRevLett.100.058001)
77. Stronge WJ. 1994 Swerve during three-dimensional impact of rough rigid bodies. *J. Appl. Mech.* **61**, 605–611. (doi:10.1115/1.2901502)
78. Gupta RK. 2021 Simulations and theory in active granular matter: nonequilibrium phase transitions and nonreciprocal interactions. PhD thesis, TIFR Centre for Interdisciplinary Sciences, India.
79. Gupta RK, Kant R, Soni H, Sood AK, Ramaswamy S. 2022 Active nonreciprocal attraction between motile particles in an elastic medium. *Phys. Rev. E* **105**, 064602. (doi:10.1103/PhysRevE.105.064602)
80. Brotto T, Caussin JB, Lauga E, Bartolo D. 2013 Hydrodynamics of confined active fluids. *Phys. Rev. Lett.* **110**, 038101. (doi:10.1103/PhysRevLett.110.038101)
81. Tjhung E, Nardini C, Cates ME. 2018 Cluster phases and bubbly phase separation in active fluids: reversal of the ostwald process. *Phys. Rev. X* **8**, 031080. (doi:10.1103/PhysRevX.8.031080)
82. Utzschneider C, Suresh B, Sciortino A, Gaillard J, Schaeffer A, Pattanayak S, Joanny JF, Blanchoin L, Théry M. 2024 Force balance of opposing diffusive motors generates polarity-sorted microtubule patterns. *Proc. Natl Acad. Sci. USA* **121**, e2406985121. (doi:10.1073/pnas.2406985121)
83. Dolai P, Simha A, Mishra S. 2018 Phase separation in binary mixtures of active and passive particles. *Soft Matter* **14**, 6137–6145. (doi:10.1039/c8sm00222c)

Downloaded from royalsocietypublishing.org/rsta/article-pdf/doi/10.1098/rsta.2025.0137/6175896/rsta.2025.0137.pdf
by Institue of Science & Technology Austria user
on 17 November 2026